EPSC2017

SB1 abstracts

EPSC Abstracts
Vol. 11, EPSC2017-143, 2017
European Planetary Science Congress 2017

Dynamics of dust particles in the Jovian gossamer rings

X. Liu (1), J. Schmidt (1) and H. Krüger (2)
(1) Astronomy Research Unit, University of Oulu, Finland (xiaodong.liu@oulu.fi), (2) Max Planck Institute for Solar System Research, Göttingen, Germany

Abstract

In this work, we analyze the dynamics of dust particles in the Jovian gossamer rings with both analytical and numerical methods. Grain sizes from submicrons to one hundred microns are considered. For the numerical simulations, high accuracy orbital integrations for the orbital evolution of dust are employed, including the effects of higher degree Jovian gravity, the Lorentz force, solar radiation pressure, Poynting-Robertson drag, plasma drag, and gravity of the Sun and the Jovian moons (the four inner Jovian moons Metis, Adrastea, Amalthea and Thebe, and the four Galilean moons Io, Europa, Ganymede and Callisto). The dust particles are started from the orbits of the Jovian moons Amalthea and Thebe. For the Jovian plasma environment, we use the new Jovian plasma model DG2 [1]. For the Jovian magnetic field, we use the field model VIPAL up to fifth degree and fifth order [2]. The details of the dynamical model for numerical simulations are described and used in [3, 4, 5]. The long-term numerical integrations are carried out in the large computer cluster located at the Finnish CSC-IT Center for Science. For micron-sized and submicron-sized particles, the precise locations of orbital resonances in the region of the gossamer rings are size-dependent. We calculate the locations of these resonances (the 1:2, 2:3, 3:4 and 4:5 exterior Lorentz resonances, the 2:1 and 3:2 Io resonances, the 1:1 Amalthea resonance, and the 1:1 Thebe resonance) with the analytical method. The resonance locations calculated with the analytical method match well with the results obtained by the simulation results. The formation of the gossamer rings and the Thebe extension can be also explained in terms of the orbital resonances of dust particles [4]. Besides, we find that a large amount of sub-micron particles are transported outward to the region of the Galilean moons.

Acknowledgements

This work was supported by the *European Space Agency* in the project Jovian Micrometeoroid Environment Model (JMEM) (contract number: 4000107249/12/NL/AF). We acknowledge *CSC – IT Center for Science* for the allocation of computational resources on their Taito cluster.

References

[1] Garrett, H. B., Kim, W., Belland, B., and Evans, R.: Jovian plasma modeling for mission design. Pasadena, CA: Jet Propulsion Laboratory, National Aeronautics and Space Administration. JPL Publication 15-11. http://hdl.handle.net/2014/45478, 2015.

[2] Hess, S. L. G., Bonfond, B., Zarka, P., and Grodent, D.: Model of the Jovian magnetic field topology constrained by the Io auroral emissions. Journal of Geophysical Research, 116, A05217, 2011.

[3] Liu, X., Sachse, M., Spahn, F., and Schmidt, J.: Dynamics and distribution of Jovian dust ejected from the Galilean satellites. Journal of Geophysical Research: Planets, 121(7):1141-1173, 2016.

[4] Liu, X., Schmidt, J., and Krüger, H.: Formation of Jupiter's gossamer rings by resonant trapping of dust. submitted to Nature Communications, 2017.

[5] Liu, X. and Schmidt, J.: An arc of dust in the region of Jupiter's Trojan asteroids. submitted to Astronomy & Astrophysics, 2017.

EPSC Abstracts
Vol. 11, EPSC2017-209, 2017
European Planetary Science Congress 2017

The role of collective self-gravity in the nonlinear evolution of viscous overstability in Saturn's rings

M. Lehmann, J. Schmidt & H. Salo
University of Oulu, Astronomy Research Unit, FI-90014, Finland (Marius.Lehmann@oulu.fi)

Abstract

We investigate the influence of collective self-gravity forces on the nonlinear, large scale evolution of the viscous overstability in Saturn's rings. We numerically solve the nonlinear hydrodynamic model equations in the isothermal and non-isothermal approximation, including radial self-gravity and employing transport coefficients derived by [3]. We concentrate on optical depths $\tau = 1.5 - 2$, which are appropriate to model Saturn's dense rings. Furthermore, local N-body simulations, incorporating vertical and radial collective self-gravity are performed. Vertical self-gravity is mimicked through an increased frequency of vertical oscillations, while radial self-gravity is approximated by solving the Poisson equation for an axisymmetric thin disk in Fourier space. Direct particle-particle forces are omitted, which prevents small scale gravitational instabilities (self-gravity wakes) from forming, an approximation that allows us to study long radial scales (5 km or more) and to compare directly the hydrodynamic model and the N-body simulations . Our isothermal and non-isothermal hydrodynamic model results, in the limit of vanishing self-gravity, compare very well with the studies of [1] and [2], respectively. In contrast, for rings with non-vanishing radial self-gravity we find that the wavelengths of saturated overstable wave trains tend to settle close to the frequency minimum of the nonlinear dispersion relation. Good agreement is found between non-isothermal hydrodynamics and N-body simulations for disks with strong radial self-gravity, while the largest deviations occur in the limit of weak self-gravity. The resulting saturation wavelengths of the viscous overstability for moderate and strong radial self-gravity ($\lambda \sim 100 - 300$m) agree reasonably well with the length scale of the axisymmetric periodic micro structure in Saturn's inner A ring and the B ring, as found by *Cassini*.

Acknowledgements

We acknowledge support from the Academy of Finland and the University of Oulu Graduate School.

References

[1] H. N. Latter and G. I. Ogilvie. Hydrodynamical simulations of viscous overstability in Saturn's rings. *Icarus*, 210:318–329, 2010.

[2] H. Rein and H. N. Latter. Large-scale N-body simulations of the viscous overstability in Saturn's rings. *MNRAS*, 431:145–158, 2013.

[3] H. Salo, J. Schmidt, and F. Spahn. Viscous overstability in Saturn's B ring: I. Direct simulations and mesurement of transport coefficients. *Icarus*, 153:295–315, 2001.

EPSC Abstracts
Vol. 11, EPSC2017-395-3, 2017
European Planetary Science Congress 2017

Large and small-scale structures in Saturn's rings

N. Albers, M.E. Rehnberg, Z.L. Brown, M. Sremčević, and L.W. Esposito
LASP, University of Colorado, Boulder, Colorado, USA (Nicole.Albers@lasp.colorado.edu)

Abstract

Observations made by the Cassini spacecraft have revealed both large and small-scale structures in Saturn's rings in unprecedented detail. Large-scale patterns include ringlets, density and bending waves, circumferential gaps, kinematic wakes, and propellers. These are foremost created by gravitational interaction with external as well as embedded moons. Analysis of Cassini and Voyager occultation data, however, revealed the presence of another moon-induced feature. Few kilometer wide individual gaps located within a few kilometers of the Encke and Keeler gap edges are exclusively found downstream of Pan and Daphnis, respectively. Recent Cassini images provide evidence for material separating from these edges, leaving depleted regions that are most likely the gaps seen in occultations.

High-resolution measurements by the Cassini Ultraviolet Spectrograph (UVIS) High Speed Photometer (HSP) and the Imaging Science Subsystem (ISS) show an abundance of intrinsic small-scale structures (or clumping), seen across the entire ring system. Examples include self-gravity wakes (50-100m), sub-km structure at the A and B ring edges, and "straw"/"ropy" structures (1-3km). In particular, wavelet analysis and an m-test based search for gaps within the A ring show that these density wakes are predominantly found in perturbed regions of the rings such as density waves and the outer A and B ring edges. Driven by resonances with external moons, these perturbed regions undergo periodic phases of compression and relaxation that correlate with the presence of structure, implying structure formation on time scales as short as one orbit. Also, double star occultations reveal radial variations at ring eges beyond the well-known large-scale excursions, that provide further evidence for the presence of intrinsic structure.

I will review observations of gaps at the Keeler and Encke gap and discuss the analysis and features of detected small-scale structures.

Acknowledgement

This work is supported by the Cassini project.

EPSC Abstracts
Vol. 11, EPSC2017-502, 2017
European Planetary Science Congress 2017

Formation of Janus and Epimetheus from Saturn's rings as co-orbitals, thanks to Mimas' 2:3 inner Mean Motion Resonances

A. Crida (1,2) and M. El Moutamid (3)
(1) Laboratoire Lagrange (UMR7293), Université Côte d'Azur / Observatoire de la Côte d'Azur, Boulevard de l'Observatoire, CS 34229, 06300 Nice, France (crida@oca.eu)
(2) Institut Universitaire de France, 103 Boulevard Saint-Michel, 75005 Paris, France
(3) Department of Astronomy, Cornell University, Ithaca, NY 14853, USA

Abstract

We show that the past confinement of Saturn's rings by Mimas' 2:3 mean motion resonances leads to the formation of two equivalent mass seeds to Janus and Epimetheus on the same orbit. This could explain the origin of their fascinating mutual horseshoe orbits configuration, in the frame of satellite formation from the spreading of the rings beyond the Roche radius [1, 3].

Figure 1: Janus and Epimetheus seen by Cassini.

1. Introduction

Janus and Epimetheus orbit Saturn at $151\,461$ km on average, on mutual horseshoe orbits with orbital separation 50 km, exchanging position every 4 years (see figure 1). This configuration is unique and intriguing : their orbital separation should converge to zero in about 20 Myrs only [4], and no satisfactory model for the origin of this co-orbital resonance exists yet. Recently, it has been demonstrated with a 1D model [1] that Janus and Epimetheus probably formed from the spreading of the rings beyond the Roche radius. However, this previous work did not address the origin of the horseshoe configuration. Here, we study this phenomenon in the frame of the elliptical restricted 3-body problem, where ring particles are perturbed by mean motion resonances with the outer satellite Mimas.

2. Our model

Two types of resonances play different roles. The Lindblad resonance (LR) confines the rings radially, and prevents their spreading. This is illustrated for instance by the confinement of the outer edge of the B-ring by Mimas' 1:2 LR (which helps preserving the Cassini division), and by the confinement of the outer edge of the A-ring by Janus' 6:7 LR [5]. In contrast, the $n:n+1$ Corotation resonance (CR) confines the rings azimuthally in n capture sites (akin Neptune's arcs).

Because of Saturn's J_2, Mimas' 2:3 CR is 130 km closer to Saturn than the 2:3 LR. Today, they are both slightly outside the Roche radius and do not interact with the rings. But Mimas is migrating outwards under the influence of the ring torque et Saturn's tides. A few hundred million years ago, both the 2:3 LR and CR with Mimas were just inside the Roche radius. At this time, the rings were confined by the 2:3 LR, and the two capture sites of the CR were full of ring material (top left panel of figure 2).

When Mimas migrated outwards so that its 2:3 mean motion resonances receded past the Roche radius, the captured material agglomerated into two bodies of $\sim 10^{15}$ kg on the exact same orbit, as sketched on top right and bottom left panels of figure 2.

These bodies then migrate outwards together due to their interaction with the rings, in mutual horseshoe orbits. The rings spawn new small satellites, eventually accreted by the proto-Janus and the proto-Epimetheus, following the pyramidal regime of the ring spreading model [3] (see the bottom right panel of figure 2). The two bodies thus grow in mass. These merging events also excite their orbital separation, leading to a configuration close to the present one.

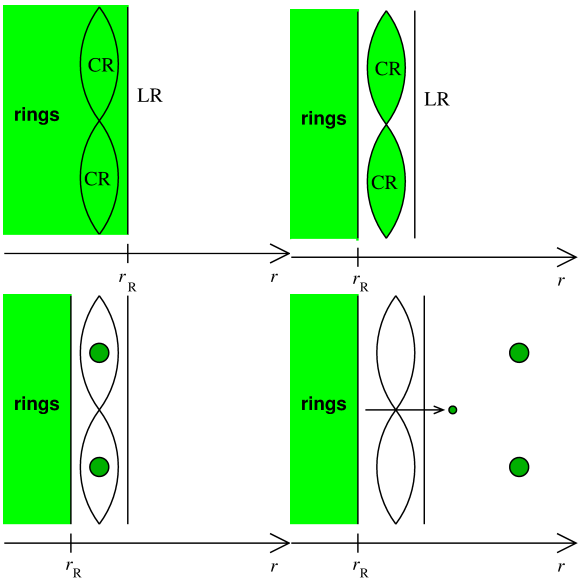

Figure 2: Sketch of our scenario for the formation of Janus and Epimetheus from the spreading of the rings
Top left : initial condition, Mimas confines the rings with it's 2:3 LR.
Top right : Mimas migrates outwards and its 2:3 mean motion resonances are now outside the Roche radius.
Bottom left : the ring material captured into the corotation sites agglomerates into 2 bodies on the same orbit.
Bottom right : the two bodies migrate outwards, while accreting satellitesimals spawn by the spreading of the rings.

3. Summary and perspective

We propose a novel solution to one of the most exciting mysteries of modern celestial mechanics : the origin of Janus and Epimetheus' mutual horseshoe configuration. In the frame of the recently developed model of formation of Saturn's regular satellites from the spreading of the rings beyond the Roche radius [1, 2, 3], Mimas' 2:3 Lindblad and Corotation resonances provide perfect conditions for the formation of 2 equal sized bodies on the same orbit.

References

[1] Charnoz, S., Salmon, J. and Crida A.: The recent formation of Saturn's moonlets from viscous spreading of the main rings, Nature, 465, pp. 752-754, 2010.

[2] Charnoz, S. et al.: Accretion of Saturn's mid-sized moons during the viscous spreading of young massive rings: Solving the paradox of silicate-poor rings versus silicate-rich moons, Icarus, 216, pp. 535-550, 2011.

[3] Crida, A. and Charnoz, S.: Formation of Regular Satellites from Ancient Massive Rings in the Solar System, Science, 338, pp. 1196-1199, 2012.

[4] Lissauer, J. J., Goldreich, P. and Tremaine, S.: Evolution of the Janus-Epimetheus coorbital resonance due to torques from Saturn's rings, Icarus, 64, pp. 425-434, 1985.

[5] El Moutamid, M. et al.: How Janus' orbital swap affects the edge of Saturn's A ring?, Icarus, 279, pp. 125-140, 2016.

EPSC Abstracts
Vol. 11, EPSC2017-563-1, 2017
European Planetary Science Congress 2017

A survey of the Saturnian ring edges: Results from double star occultations

N. Albers and M. Sremčević
LASP, University of Colorado, Boulder, Colorado, USA (Nicole.Albers@lasp.colorado.edu)

Abstract

The Cassini Ultraviolet Imaging Spectrograph (UVIS) High Speed Photometer (HSP) has recorded more than 150 stellar occultations of Saturn's rings. About one third of these are observations involving double stars, where each star contributes its own, independent light curve. For each light curve its footprint, as projected into the ring plane and dependent on observation geometry, samples a different region in the ring. Here, we focus on ring edges. Each occultation then yields two independent edge measurements at two different times and longitudes. We infer relative changes in optical depth and radial position over an azimuthal distance as short as 20 meters. These relative measurements require neither photometric nor geometric calibration and inform on the small-scale variability of structure/features with relative resolutions an order of magnitude higher than typically achieved.

The Encke and Keeler gap edges as well as the outer B and A ring edges show radial excursions on the order of tens of meters. These radial variations are, in comparison to the common multi-mode analysis of edge kinematics, high-frequency components with corresponding m numbers of m>5000000. We note that spatial dimensions inferred here are 10-100 times smaller than those of features Region A and B at the B ring edge or "Peggy"-type objects at the A ring edge, and are comparable to individual self-gravity wakes or clumps/particles. The Titan and Huygens ringlets inner and outer edges, on the other hand, are, in comparison, highly regular and smooth with radial variations of only a few meters. Nevertheless they show variations in normal optical depth on the order of 0.4, well above the expected margin due to intrinsic stellar variability. We also identified three features in the C ring that show little radial variability and can thus be considered smooth. Interestingly, this irregularity or raggedness of the edges - manifestation of intrinsic small-scale structure of the ring - is stronger with increasing radial distance from Saturn. This is consistent with the current understanding that larger structures form in regions of weaker tidal forces or perturbed regions such as the A and B ring edges.

Acknowledgement

This work is supported by the Cassini project.

EPSC Abstracts
Vol. 11, EPSC2017-590-1, 2017
European Planetary Science Congress 2017

Dust characteristics of dusty plasma ring of Saturn

M. W. Morooka (1), J.-E. Wahlund (1), S.-Y. Ye (2), A. M. Persoon (2), and W. S. Kurth (2)
(1) Swedish Institute of Space Physics (IRFU), Uppsala, Sweden, (2) Department of Physics and Astronomy, University of Iowa, Iowa City, IA, USA (morooka@irfu.se)

Abstract

During the Ring Grazing orbit, starting from December 2016, Cassini carried out twenty of the faint Saturn ring crossing observations at the distance of 2.45-2.51 R_S ($1R_S \sim 60{,}268$ km) from Saturn center. We will show the electron and the ion density measurements of the RPWS/Langmuir Probe (LP) during these orbits. In most of the orbits significant ion/electron density differences have been observed, which indicates the presence of the charged nm and μm sized grains. The relationship between the observed charge densities and the electrical potential of the grains shows that the grains and the ambient electrons and ions are electro dynamical ensemble, a dusty plasma. The results show that characteristic dust size changes depending on the distance from the ring center. The result suggests that a dusty plasma state is related to the dynamics of the grain sizes.

1. Introduction

Near the Enceladus and its surrounded E ring Cassini observations revealed that the nm and μm sized charged dust grains are abundant and playing an important role in the plasma dynamics; the dusty plasma [1], [2]. In such region, a large unbalance of the ion and the electron densities (the ion density higher than the electron density) had been observed. Dusty plasma can be expected in other place of the ring system, especially in the faint rings that is composed of nm and μm size small grains such as the F ring [3].

2. Results

Series of the ring passage observation show a consistent dust and plasma structure around the equator:

1) Relatively dense plasma disk has been observed in both the electron and the ions around the equator at $|Z_{KME}|<1R_S$.

2) An additional sharp ion density increasing has been observed at $|Z_{KME}|<0.1R_S$. The observed densities at the equator were several 10^2 cm^{-3} for ions, while the electron density remains a few 10 cm^{-3}. The density ratio of the electrons to the ions (Ne/Ni) were close to or less than 0.1 at the equator.

3) The μm sized dust density enhancement has been observed in the region. However, the region was narrower ($|Z_{KME}|<0.02R_S$) than the ion density enhancement region. This suggests that the characteristic size of the negative charged particles varies depending on the distance from the ring center. On the other hand, the dominant part of the negative charges is carried by the nm size small grains in all the region where the electron/ion density difference have been observed.

5) The density ratio of the electrons to the ions has variations over the five months of Dust Grazing orbits. It had decreasing variation in the first eight Dust Grazing orbits (the orbit 251, doy339 2016 to the orbit 258, doy023 2017), and then sharply increased at orbit 267 and in a decreasing phase again.

In addition, the plasma wake effect has been observed in a few orbits when the LP is located in the downstream of the ideal co-rotation of the spacecraft, which means that the observed LP current are not due to the secondary effect of the dust but the plasma ions flowing around the spacecraft.

The observed plasma and dust parameters are important not only in suggesting the presence of the dusty plasma near the F ring, but also showing an importance of the small nm size grains as a negative charge carrier in a dusty plasma [4], [5]. Numbers of close optical investigations of F rings by Cassini showed the highly variable F ring structure that is affected by the orbits of the nearby object [6] and the dust size characteristics are also variable in different region. The relationship of the dust size distribution and the dust state obtained here implies a complex

dusty plasma dynamics related to the dynamics of the grain aggregation and the shattering processes.

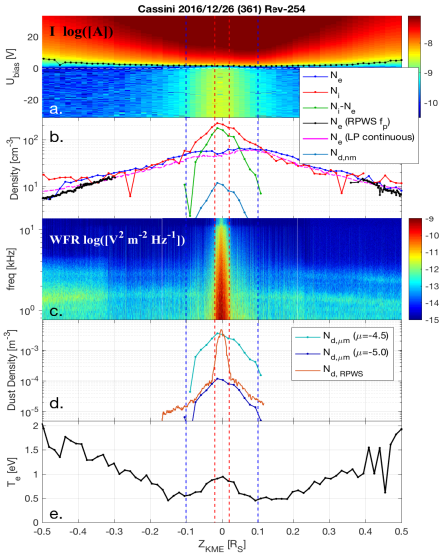

Figure 1: The summary of the Langmuir probe observation during one of the ring crossing. Panels show from the top: VI spectrogram of the LP, the densities of the charged particles, µm sized dust observation of RPWS, the estimated µm sized grain density, and the electron temperature.

References

[1] Wahlund, J.-E. et al. (2009), Detection of dusty plasma near the E-ring of Saturn, Planet Space Sci, 57(1), 1795–1806, doi:10.1016/j.pss.2009.03.011.

[2] Morooka, M. W., J.-E. Wahlund, A. I. Eriksson, W. M. Farrell, D. A. Gurnett, W. S. Kurth, A. M. Persoon, M. Shafiq, M. André, and M. K. G. Holmberg (2011), Dusty plasma in the vicinity of Enceladus, Journal of Geophysical Research, 116(A12), A12221–, doi:10.1029/2011JA017038.

[3] Goertz, C. K. (1984), Formation of Saturn's spokes, Advances in Space Research, 4(9), 137–141, doi:10.1016/0273-1177(84)90018-8.

[4] Meyer-Vernet, N., 2013. On the charge of nanograins in cold environments and Enceladus dust. *Icarus*, 1306, pp.583–590. Available at: http://www.elsevier.com/locate/icarus.

[5] Yaroshenko, V.V., Lühr, H. & Miloch, W.J., 2014. Dust charging in the Enceladus torus. *Journal Of Geophysical Research-Space Physics*, 119(1), pp.221–236. Available at: http://doi.wiley.com/10.1002/2013JA019213.

[6] Cuzzi, J. et al., 2009. Ring Particle Composition and Size Distribution. , p.459. Available at: http://adsabs.harvard.edu/cgi-bin/nph-data_query?bibcode=2009sfch.book..459C&link_type=ABSTRACT.

EPSC Abstracts
Vol. 11, EPSC2017-675, 2017
European Planetary Science Congress 2017

N-body modeling of viscous overstability in Saturn's rings

H. Salo
Univ. of Oulu, Finland (heikki.salo@oulu.fi)

Abstract

The viscous overstability of dense planetary rings is a promising mechanism for the generation of observed 100-200 meter radial density variations in the B and the inner A ring of Saturn, detected by Cassini RSS, UVIS, and VIMS occultations [1, 7, 2]. Viscous overstability, in the form of spontaneous growth of axisymmetric oscillations, arises naturally in N-body simulations in the limit of high impact frequency and moderately weak selfgravity [3, 4, 5, 6]. The basic mechanism behind this instability mechanism is the rapid rise of viscosity with density, leading to a situation where collisional flux overshooths in trying to smooth the density variations.

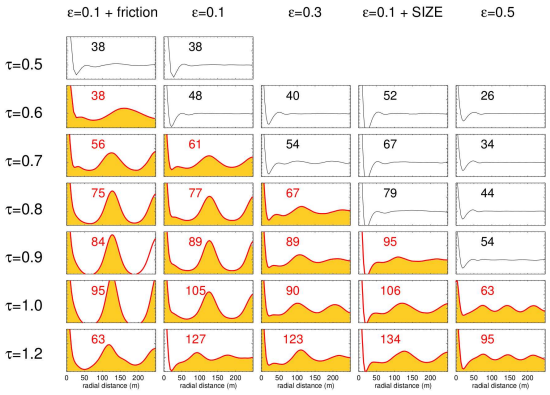

Figure 1: Survey of the onset of viscous overstability in N-body simulations with different dynamical optical depths τ and particle elastic properties (ϵ denotes the normal coefficient of restitution). The time-averaged radial cuts of the particle-particle autocorrelation function are displayed: regular undulations indicate the presence of overstable oscillations (highlighted by orange color). The labels indicate the impact frequency (imapact/particle/orbit). It is seen that increased dissipation promotes overstability.

This presentation reviews the N-body modeling of overstability, and whenever possible, ties the numerical results to Cassini observations. In particular we address the threshold optical depth for obtaining overstability, and how this depends on particle physical properties (see Fig. 1). The differences between non-gravitating simulations, and simulations including ring self-gravity with various degrees of approximations are also addressed.

Acknowledgements

This study is supported by the Academy of Finland

References

[1] Colwell, J. E., Esposito, L. W., Sremčević, M., Stewart, G. R., and McClintock, W. E. (2007). Self-gravity wakes and radial structure of Saturn's B ring. *Icarus*, 190:127–144.

[2] Hedman, M. M., Nicholson, P. D., & Salo, H. 2014, *AJ*, 148, 15

[3] Salo, H., Schmidt, J., and Spahn, F., 2001. Viscous overstability in Saturn's B-ring: I. Direct simulations and measurement of transport coefficients. Icarus, 153, 295–315.

[4] Schmidt, J., Salo, H., Spahn, F., and Petzschmann, O. (2001). Viscous overstability in Saturn's B ring: II. Hydrodynamic theory and comparison to simulations. *Icarus*, 153:316–331.

[5] Schmidt, J. and Salo, H. (2003). A weakly nonlinear model for viscous overstability in saturn's dense rings. *Physical Review Letters*, 90(6):061102.

[6] Schmidt, J., Ohtsuki, K., Rappaport, N., Salo, H., Spahn, F., 2009. Dynamics of Saturn's dense rings. In: Brown, R.H., Dougherty, M. (Eds.), Saturn after Cassini-Huygens. Kluwer, pp. 413-458.

[7] Thomson, F. S., Marouf, E. A., Tyler, G. L., French, R. G., and Rappoport, N. J. (2007). Periodic microstructure in Saturn's rings A and B. *Gephys. Res. Lett.*, 34:24203.

EPSC Abstracts
Vol. 11, EPSC2017-677, 2017
European Planetary Science Congress 2017

Analyzing Blériot's propeller gaps in Cassini NAC images

H. Hoffmann (1), C. Chen (2), M. Seiß (1), N. Albers (3), and F. Spahn (1)
(1) Institute of Physics and Astronomy, University of Potsdam, Germany (hohoff@uni-potsdam.de), (2) Department of Physics and Astronomy University of Nevada, Las Vegas, USA (3) LASP, University of Boulder, Colorado, USA.

Abstract

Among the great discoveries of the Cassini mission are the propeller-shaped structures created by small moonlets embedded in Saturn's dense rings. These moonlets are not massive enough to counteract the viscous ring diffusion to open and maintain circumferential gaps, distinguishing them from ring-moons like Pan and Daphnis.

Partial gaps are one of the defining features of propeller structures. Until recently only the largest known propeller named Blériot showed well-formed partial gaps in images taken by the Narrow Angle Camera onboard the Cassini spacecraft [1]. We analyze images of the sunlit side of Saturn's outer A ring which show the propeller Blériot with clearly visible gaps. By fitting a Gaussian to radial brightness profiles at different azimuthal locations, we obtain the evolution of gap minimum and gap width downstream of the moonlet.

We report two findings:

1. Numerical simulations indicate that the radial separation of the partial propeller gaps is expected to be 4 Hill radii [1, 2, 3]. From the radial separation of the gaps in the analyzed images, we infer Blériot's Hill radius to be a few hundred meters, consistent with values given by [4, 5, 6].

2. In order to estimate the ring viscosity in the region of Saturn's outer A ring, where Blériot orbits, we fit several model functions (one example being the analytic solution derived in [7]), which describe the azimuthal evolution of the surface density in the propeller gap region, to the data obtained from the image analysis. We find viscosity values consistent with the parameterization of ring viscosity by [8], but significantly lower than the upper limit given by [9].

[1] Recently, partial gaps were also resolved for the propellers Earhart and Santos-Dumont in high resolution images taken during Cassini's *ring grazing orbits.*

References

[1] Spahn, F. and Sremčević, M.: Density patterns induced by small moonlets in Saturn's rings?, A&A, Vol. 358, pp. 368-372, 2000.

[2] Seiß, M., Spahn, F., Sremčević, M., and Salo, H.: Structures induced by small moonlets in Saturn's rings: Implications for the Cassini Mission, GeoRL, Vol. 32., L11205, 2005.

[3] Lewis, M. C. and Stewart, G. R.: Features around embedded moonlets in Saturn's rings: The role of self-gravity and particle size distributions, Icarus, Vol. 199, pp. 387-412, 2009.

[4] Sremčević, M., Stewart, G. R., Albers, N., and Esposito, L. W.: Propellers in Saturn's rings, European Planetary Science Congress, Vol. 9, id. EPSC2014-633, 2014.

[5] Hoffmann, H., Seiß, M., Salo, H., and Spahn, F.: Vertical structures induced by embedded moonlets in Saturn's rings, Icarus, Vol. 252, pp. 400-414, 2015.

[6] Seiß, M., Albers, N., Sremčević, M., Schmidt, J., et al.: Hydrodynamic simulations of moonlet induced propellers in Saturn's rings: Application to Blériot, arXiv:1701.04641, 2017.

[7] Sremčević, M., Spahn, F., and Duschl, W. J.: Density structures in perturbed thin cold discs, MNRAS, Vol. 337, pp. 1139-1152, 2002.

[8] Daisaka, H., Tanaka, H., and Ida, S.: Viscosity in a Dense Planetary Ring with Self-Gravitating Particles, Icarus, Vol. 154, pp. 296-312, 2001.

[9] Esposito, L. W., O'Callaghan, M., and West, R. A.: The structure of Saturn's rings - Implications from the Voyager stellar occultation, Icarus, Vol. 56, pp. 439-452, 1983.

EPSC Abstracts
Vol. 11, EPSC2017-810, 2017
European Planetary Science Congress 2017

In-situ dust measurements during Cassini's F-ring and proximal orbits

R. Srama (1, 2) for the CDA Science Team
(1) University Stuttgart, Germany, (2) Baylor University, Waco, TX, USA (srama@irs.uni-stuttgart.de)

Abstract

The Cosmic Dust Analyzer (CDA) onboard Cassini characterized successfully the dust environment at Saturn since 2004. The instrument measured the primary charge, speed, mass and composition of individual submicron and micron sized dust grains. Starting in December 2016 Cassini performed ring plane crossings at radial distances of 2.48 Saturn radii and at 1.05 Saturn radii (proximal orbits, starting in April 2017). For the first time, an in-situ dust detector explored the F-ring region of Saturn. CDA determined particle densities, particle mass distributions and compositional measurements. Furthermore, the High Rate Detector (HRD) was activated using a high time and spatial resolution. The relativ impact speed of dust grains at the instrument target during ring plane crossings was 20 km/s (F ring orbits) and 30 km/s (proximal orbits), respectively. The high impact speeds allowed a sensitive compositional analysis and the detection of grains well below 50 nm. CDA successfully characterized the F-ring region and found, that the inner edge of the E-ring reaches radial distances of 2.5 Rs. Larger grains above 0.8 micron are focused to the ring plane, whereas smaller grains were measured as far as 60.000 km away from the ring plane.
For the first time, in-situ measurements were performed inside Saturn's main ring system at radial distances of 1.05 Saturn radii. The overall dust density within Saturn's main ring and close to Saturn is much lower than expected. Especially larger grains above 0.7 micron are depleted. The characterization of the "ring rain" from Saturn's main ring towards Saturn was an ultimate goal of CDA.

EPSC Abstracts
Vol. 11, EPSC2017-845, 2017
European Planetary Science Congress 2017

Formation of moon induced gaps in dense planetary rings

F. Grätz, M. Seiß and F. Spahn, Institut für Physik und Astronomie, Universität Potsdam, Germany,
fgraetz@uni-potsdam.de

Abstract

Discs are a common structure in the universe that appears on a vast range of different size scales: Galaxies, active galactic nuclei, protoplanetary discs, solar systems and planetary rings. Recent works have shown that bodies embedded in protoplanetary discs or planetary rings create S-shaped density modulations called propellers if their mass deceeds a certain threshold or cause a gap around the entire circumference of the disc if the embedded bodies mass exceeds it. Two counteracting physical processes govern the dynamics and determine what structure is created: The gravitational disturber excerts a torque on nearby disc particles, sweeping them away from itself on both sides thus depleting the discs density and forming a gap. Diffusive spreading of the disc material due to collisions counteracts the gravitational scattering and has the tendency to fill the gap. Propeller structures where predicted and discussed in detail by Spahn and Sremčević [1, 2] and were later discovered by the Cassini spacecraft [3, 4, 6, 5]. Cassini found the tiny moon Daphnis in the Keeler division [7] and just recently the ALMA radio telescope for the first time discovered gaps in a protoplanetary disc [8] thus might have indirectly whitnessed the birth of protoplanets.

We develop a nonlinear diffusion model that accounts for those two counteracting processes and describes the azimutally averaged surface density profile an embedded moon creates in planetary rings. The gaps width depends on the moons mass, its radial position and the rings viscosity allowing us to estimate the rings viscosity in the vicinity of the Encke and Keeler gap in Saturns A-Ring and compare it to previous measurements [9, 10]. We show that for the Keeler gap the time derivative of the semi-major axis as derived by [11] ($\frac{\mathrm{d}a}{\mathrm{d}t} \sim \frac{1}{x^4}$) is underestimated yielding an underestimated viscosity for the ring. We therefore derive a corrected expression for said time derivative by fitting the solutions of Hill's equations for an ensemble of test particles. Furthermore we estimate the masses for potentionally unseen moonlets in the C-Ring and Cassini division.

References

[1] Spahn, F., Sremčević, M.: Density patterns induced by small moonlets in Saturn's rings?, Astronomy and Astrophysics, Vol. 358, pp. 368-372, 2000

[2] Sremčević, M., Spahn, F., Duschl, W.: Density structures in perturbed thin cold discs, Monthly Notices of the Royal Astronomical Society, Vol. 337, pp. 1139-1152, 2002

[3] Tiscareno, M. S., Burns, J. A., Hedman, M. M., Porco, C. C., Weiss, J. W., Dones, L., Richardson, D. C., Murray, C. D.: 100-metre-diameter moonlets in Saturn's A ring from observations of 'propeller'structures, Nature, Vol. 440, pp. 648-650, 2006

[4] Sremčević, M., Schmidt, J., Salo, H., Seisz, M., Spahn, F., Albers, N.: A belt of moonlets in Saturn's A ring, Nature, Vol. 449, pp. 1019-1021, 2007

[5] Tiscareno, M. S., Burns J. A., Hedman, M. H., Porco, C. C.: The Population of Propellers in Saturn's A Ring, The Astronomical Journal, Vol. 135, pp. 1083, 2008

[6] Tiscareno, M. S., Burns, J. A., Sremčević, M., Beurle, K., Hedman, M. H., Cooper, N. J., Milano, A. J., Evans, M. E., Porco, C. C., Spitale, J. N., Weiss, J. W.: Physical Characteristics and Non-Keplerian Orbital Motion of "Propeller" Moons Embedded in Saturn's Rings, The Astrophysical Journal Letters, Vol. 718, L92, 2010

[7] Porco, C. C.: S/2005 S 1, IAU Circulars, Volume 8524, p. 1., 2005

[8] Hsi-Wei Yen and Hauyu Baobab Liu and Pin-Gao Gu and Naomi Hirano and Chin-Fei Lee and Evaria Puspitaningrum and Shigehisa Takakuwa: Gas Gaps in the Protoplanetary Disk around the Young Protostar HL Tau, The Astrophysical Journal Letters, Vol. 820, L25, 2016

[9] Tiscareno, M. S., Burns, J. A., Nicholson, P. D., Hedman, M. H., Porco, C. C.: Cassini imaging of Saturn's rings: II. A wavelet technique for analysis of density waves and other radial structure in the rings, Icarus, Vol. 189, pp. 14-24, 2007

[10] Tajeddine, R., Nicholson, P. D., Tiscareno, M. S., Hedman, M. H., Burns, J. A., El Moutamid, M.: Dynamical phenomena at the inner edge of the Keeler gap, Icarus, Vol. 289, pp. 80-93, 2017

[11] Goldreich, P., Tremaine, S.: Disk-satellite interactions, Astrophysical Journal, Vol. 241, pp. 425-441, 1980

EPSC Abstracts
Vol. 11, EPSC2017-853, 2017
European Planetary Science Congress 2017

Studies of asymmetric propeller structures in the Saturnian ring system

Michael Seiler, Martin Seiß, and Frank Spahn
Departement of Physics and Astronomy, University of Potsdam, Germany (miseiler@uni-potsdam.de)

Abstract

Small sub-kilometer sized objects (called moonlets) embedded in the dense rings of Saturn cause density structures due to their gravitational interaction with the surrounding ring material which resemble a propeller, giving the structure its name. The prediction of the existence of propeller structures within the dense rings of Saturn [2, 3] led to their detection [5, 4, 6]. The recurrent observation of the largest propeller structure called Blériot in Cassini ISS images allowed the reconstruction of its orbit. The analysis yielded that Blériot is deviating considerably from its expected Keplerian orbit [7]. This offset motion can be astonishlingly well composed by a three-mode hamonic fit [1].

We perform hydrodynamic simulations to study the changes of the propeller structure due to a disk-embedded moonlet which is librating in a certain mode around its mean position. We present results showing how the induced propeller structure changes due to the libration of the moonlet and if these changes are visible in Cassini images. Further, we estimate the influence of the gap's gravity on the moonlet. In this way, we test the model of Seiler et al. (2017), who predict the moonlet to librate around its mean position due to the back reaction of the gap on the moonlet [1].

Acknowledgements

This work has been supported by the Deutsche Forschungsgemeinschaft (Sp 384/28-1) and the Deutsches Zentrum für Luft-und Raumfahrt (OH 1401).

References

[1] Seiler, M. et al., A Librational Model for the Propeller Blériot in the Saturnian Ring System, ArXiv e-prints, 2017.

[2] Spahn, F. and Sremčević, M., Density patterns induced by small moonlets in Saturn's rings?, Astronomy and Astrophysics, 358, 368–372.

[3] Sremčević, M. et al., Density structures in perturbed thin cold discs, Monthly Notices Royal Astron. Soc., 337, 1139–1152.

[4] Sremčević, M. et al., A belt of moonlets in Saturn's A ring, Nature, 449, 1019–1021.

[5] Tiscareno, M. S. et al., 100-metre-diameter moonlets in Saturn's A ring from observations of "propeller" structures, Nature, 440, 648–650.

[6] Tiscareno, M. S. et al., The Population of Propellers in Saturn's A Ring, Astronomical Journal, 135, 1083–1091.

[7] Tiscareno, M. S. et al., Physical Characteristics and Non-Keplerian Orbital Motion of "Propeller" Moons Embedded in Saturn's Rings, Astrophysical Journal Letters, 718, pp. L92-L96, 2010.

EPSC Abstracts
Vol. 11, EPSC2017-854, 2017
European Planetary Science Congress 2017

Near-infrared spectra of Saturn's ring spokes from Cassini-VIMS data

E. D'Aversa (1), G. Bellucci (1), G.Filacchione (1), P.Cerroni (1), P.D.Nicholson (2), F.G.Carrozzo (1), F.Altieri (1), F.Oliva (1), A.Geminale (1), G.Sindoni (1), and M.M.Hedman (3)

(1) IAPS-INAF, Istituto di Astrofisica e Planetologia Spaziali, Rome, Italy, (2) Cornell University, Ithaca, NY, USA, (3) University of Idaho, Moskow, USA (emiliano.daversa@iaps.inaf.it / Fax: +39-06-45488383)

Abstract

Saturn's ring spokes are still a not fully understood phenomenon, observed so far only during the three Saturnian equinoxes in the space era (every ~14 years). Cassini-VIMS observations during the 2009 equinox widened for the first time the spoke investigations to the near-infrared spectral range longward of 1 μm. Two sets of spoke sequences, at different solar phase angles, will be discussed here. The coverage of water ice and methane absorption bands of the VIMS spectra seems to suggest that further illumination sources other than direct sunlight are significant in producing the observed spoke reflectance, and the consequences for microphysics retrievals will be discussed.

1. Introduction

Saturn's B ring is known to sometime host some elongated ephemeral features appearing close to the Saturnian equinoxes. They have been imaged in the past in only three occasions: during 1980 equinox by Voyager cameras [1], during 1995 equinox through Hubble Space Telescope [2], and during 2009 equinox by Cassini camera [3]. Images showed spokes being darker than the ring at small solar phase angles and brighter at high phase angles. Moreover they move partially pushed by Saturn's magnetic field, suggesting that they are composed of very small charged dust/ice grains.

Physical models, based on electrostatic lifting of fine sub-micron grains from the regolith of ring's particles, have been developed since Voyager observations. However, there is not yet unanimous consensus on the formation mechanisms for spokes, in particular about the triggering process. Meteoroids bombardment has been earlier invoked as trigger ([4]), as well as precipitation of electrons from Saturn's lightning storms ([5]), while collisional cascade models have been proposed to trigger the formation of spokes from the debris of other spokes ([6]). In any case, the dynamical evolution of spoke's grains is driven by their mass and their charge, and both these parameters are rather poorly constrained by observations.

1.1 Spokes by Cassini-VIMS

Cassini mission allowed for the first time to observe spokes in the near-infrared, by means of the *Visual and Infrared Mapping Spectrometer* (VIMS). This is an imaging spectrometer providing data cubes in the 0.35-5.1 μm range with a 7 to 20 nm spectral resolution, and able to acquire images of the Saturn's ring with discrete flexibility in terms of spatial resolution, phase angle, and pointing. Dozens of spokes are detectable in VIMS images acquired for several months across the 2009 August equinox. They allow unprecedented studies on their spectral properties, with the purpose of retrieving composition and structure of spoke grains from the way they modify the B ring reflectance. Earliest analysis of this data suggested the presence in spokes of a population of micron-sized grains larger than previously thought ([7]). However, the retrieval of spoke properties from spectra is not straightforward as they act as a small perturbation of the ring's reflectance, often smaller than the strong radial variation of B ring. At the VIMS moderate spatial resolution, spokes often cover an unknown fraction of few VIMS pixels.

2. VIMS spectra of spokes

We will report here about two significant VIMS-IR spoke datasets (0.8-2.8 μm), acquired at very different solar phase angles, showing two sequences of bright and dark spokes.

A bright spokes sequence (figure 1) has been identified in a long staring data sequence of images at high phase angle (110°), where at least 7/8 spatially unresolved spokes can be found shining against a dark B ring. A dark spokes sequence (figure 2) has been found by mosaicking a low phase angle (40°) data sequence at much higher spatial resolution. Both sequences have been acquired by staring pointing to the morning ring ansa for a duration long enough to cover about one full rotation of Saturn.

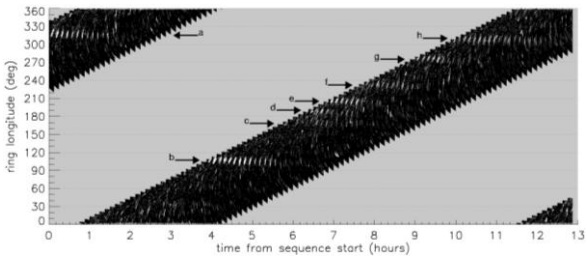

Figure 1: a sequence of bright spokes extracted from a VIMS data sequence at 110° phase angle.

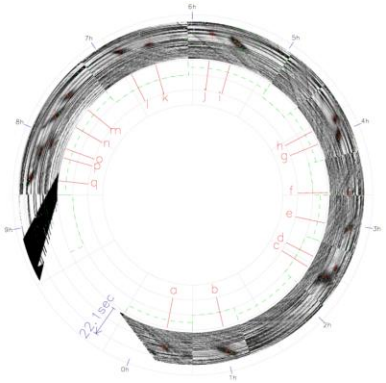

Figure 2: a sequence of dark spokes in a mosaic of VIMS data at 40° phase angle.

3. Multiple reflections

In the observing condition of the bright spokes sequence, the light scattered by the rings appear strongly contaminated by the illumination from Saturn (Saturn-shine), and this is particularly true for the B ring. Even when B ring reflectance is removed, bright spokes spectra clearly show reversed residual methane bands suggesting the spokes would be dark if viewed in Saturn's light only. Moreover, the spectra over both bright and dark spokes show enhanced water ice absorption bands in respect to the B ring in the same observing conditions. At the current stage of analysis, the most likely explanation invokes ring-shine as a further illumination source, able to directly enhance the water ice signatures, as observed.

4. Summary and conclusions

Detection of multiple illumination sources for spokes other than direct sunlight is discussed. VIMS is the first instrument sensitive to these multiple shines on spokes thanks to the coverage of near infrared range. However these multiple shines can also affect the visible wavelength range, where all the results from previous studies about spokes microphysics rely, and where these effects are hardly recognizable. As a consequence, previous retrieval of spoke properties based on visible observations may be somewhat biased. De-biased retrievals require more complex models of radiative transfer, but may yield to spoke particles more isotropically scattering than previously thought, possibly confirming the higher concentration of μm-sized particles as suggested in [7].

Acknowledgements

This work has been supported by Italian Space Agency (ASI) through Cassini contract.

References

[1] Smith et al.,1981,Science,212,163.

[2] McGhee et al.,2005,Icarus,173,508.

[3] Mitchell et al.,2013,Icarus,225,446.

[4] Morfill&Thomas,2005,Icar,179,539.

[5] Jones et al.2006,GRL,33,L21202.

[6] Hamilton&Jontof-Hutter,2014,AGUFM.P11B3759H.

[7] D'Aversa et al.,2010,GRL,37,GL041427.

EPSC Abstracts
Vol. 11, EPSC2017-943, 2017
European Planetary Science Congress 2017

Planetary Rings: Deviation from Energy-Equipartition the Temperature-Vector

F. Spahn, Y. Baibolatov, and E. Seyfarth
– Institute of Physics & Astronomy, Univ. Potsdam, D-14476 Potsdam, GERMANY,

Abstract

Planetary rings are ensembles of granular (icy) aggregates ranging in size from centimetres up to a few metres. They form an extremely thin Keplerian disk – vertical extent of about 10 metres – driven by a steady shear caused by the gravity of the central planet. The ensemble is dominated by dissipative collisions which, in densest regions of Saturn's rings, reach more than $> (3\Omega\tau)^{-1}$ collisions per orbital period $T = 2\pi/\Omega$ (Kepler-orbital frequency Ω). The optical depth $\tau \propto \sigma$ is a measure for the surface-mass density σ in the rings. Each collision is able to either dissipate thermal energy of the ring-aggregates while it may change its size due to aggregation or fragmentation [1]. A balance between aggregation and fragmentation has found to successfully explain the observed size distribution of e.g. Saturn's rings [2] under assumptions of Maxwellian velocity distribution (VD) and energy-equipartition in form of an unique granular temperature T characteristic for all particles sizes k (k – number of model-monomers the aggregated consist of).

However, an expression of the deviation from the thermodynamic equilibrium of the ensemble – irreversible collisional processes dissipate kinetic (thermal) energy of the ensemble – is the violation of the energy equipartition. The latter is characteristic for conservative Hamiltonian systems.
In this work we quantify this effect by describing a balance between granular cooling $\propto (1-\epsilon^2)$ and viscous heating $\propto \nu\Omega^2$, again under the assumption of Gaussian VD, but with *mass dependent* granular temperatures $T(k) = T_k$. Here, the restitution coefficient ϵ (ratio of the normal impact speed before and after the collision) is assumed to be rather small $\epsilon \ll 1$ and constant, while ν labels the granular viscosity. Using the momentum-conservation and the energy-balance at a single binary collision between a small (mass m_s) and a large (mass m_l) we show that the respective specific energy-dissipation $\Delta E_{s/l} \propto m_{s/l}/(m_s + m_l)$ is the larger the smaller the ring-aggregate is. In other words, the deviation from the energy equipartition becomes largest for the smalles members of the aggregate ensemble. We quantify this effect in a steady state by using the mass/size distribution $n_k = n(k)$ derived by Brilliantov et al. [2].

The extension of the state variables a temperature vector T_k, in addition to mass-densities ϱ_k and velocities $\vec{u}_k \approx \vec{u}$, allows to charactize the mass/size dependence of transport-processes (e.g. $\nu \rightarrow \nu_k$). This offers the chance to investigate possible related instabilites like e.g. mass seggregation, clustering.

References

[1] Spahn, F., Albers, N., Sremcevic, M., and Thornton, C. 2004. Kinetic description of coagulation and fragmentation in dilute granular particle ensembles. *Europhys. Lett.*, **67**, 545–551.

[2] Brilliantov, N. V., Krapivsky, P. L., Bodrova, A., Spahn, F., Hayakawa, H., Stadnichuk, V., and Schmidt, J. 2015. Size distribution of particles in Saturn s rings from aggregation and fragmentation. *PNAS*, **112**, 9536–9541.

EPSC Abstracts
Vol. 11, EPSC2017-953, 2017
European Planetary Science Congress 2017

In situ survey of micron-sized dust at Saturn by using the HF radio antennas : application to Cassini Grand Finale orbits

M. Moncuquet, M. Pallu, K. Issautier
LESIA, CNRS - Observatoire de Paris, Meudon, France (michel.moncuquet@obspm.fr)

Abstract

In order to create an in-situ survey of the microsized dust in the inner magnetosphere of Saturn, we used a new method, applied to a collection of about one million radio spectra acquired between 2004 and 2016 with the HF-RPWS receiver (covering the band 3.5-318 kHz [2]), simultaneously with two kinds of electric antennas, a monopole and a dipole (paper in preparation 2017).

The method consists in the comparison of the voltage power spectra measured from the monopole and from the dipole, and then exploiting the fact that the monopole is much more sensitive to the dust impacts than the dipole [1]. For that purpose, we are using the lowest band of the HF-RPWS receiver (3.5kHz-10kHz), where both the plasma shot noise and the dust impact noise are fully dominant. We obtain a reliable diagnosis on the dust grains impacting the spacecraft, namely an *observable* which is only depending on the ambient dust grain density, grains size distribution and their impact velocities.

The main advantages of the method is to allow, with rather small telemetry flow, a continuous survey of the dust impacting the spacecraft. The dust observable is almost immune to the spacecraft floating potential and practically uncorrelated to the ambient plasma variations, in addition to having a large impact detection area and a high cadence of measurements.

The main inconvenience is to supply only one observable which is a mixing between a minimal dust flux (with a threshold of sensitivity) and the mass/size of grains, including some assumptions about dust impact velocities on the Cassini spacecraft. Since this technique reveals the dust concentration together with the electron density and temperature, with the same instrument, it is also particularly suitable to study dust-plasma interactions.

Over a long period of observations on many Cassini's orbits, it has revealed the long-term and large-scale structure of the dust distribution in the innermost part of the visited Saturn's magnetosphere, in a very reliable way from about 2 to 13 Rs, that is within the dust E-ring and the plasma torus (both originating from Enceladus cryovolcanic activity).

In this presentation, we will show the more recent results obtained with our method and we will eventually focus on the data acquired during the Cassini Grand Finale. The dusty plasma diagnosis should be relevant around each crossings of the ring plane, at about 1Rs from Saturn and $\pm 10\,\mathrm{deg}$ latitude. We plan to discuss some properties of the dust which populates (or not) the equatorial plane between the inner edge of the rings and the upper ionosphere of Saturn.

References

[1] Meyer-Vernet, N., Moncuquet, M., Issautier, K., Lecacheux, A.: The importance of monopole antennas for dust observations: why Wind/WAVES does not detect nanodust, Geophys. Res. Lett., 41, doi:10.1002/2014GL059988, 2014.

[2] Gurnett, D. A., et al.: The Cassini Radio and Plasma Wave Investigation, Space Sci. Rev., Volume114, pp. 395-463, 2004.

EPSC Abstracts
Vol. 11, EPSC2017-996, 2017
European Planetary Science Congress 2017

Imaging of Saturn's main rings during the Cassini Ring-Grazing Orbits and Grand Finale

Matthew S. Tiscareno (1) for the Cassini Imaging Team
(1) Carl Sagan Center for the Study of Life in the Universe, SETI Institute, Mountain View CA, USA (matt@seti.org)

Abstract

In its two-part end-of-mission maneuvers, the Cassini has obtained and (as of this writing) continues to obtain the sharpest and highest-fidelity images ever taken of Saturn's rings. Among the results we can report so far are 1) radial variations in the degree of visible "clumpiness" in the ring, 2) a particle-size distribution for small "propellers," yielding insights into the history and dynamics of the ring's largest particles, 3) close-range flybys of three large "propellers," obtaining new details of how the unseen moons disturb and interact with the ring in which they are embedded, and 4) expanded data on the size, frequency, and spectral properties of impact ejecta clouds in the rings.

We will report on our ongoing analysis of these new images.

1. Introduction

Cassini is ending its spectacular 13-year mission at Saturn with a two-part farewell. From December 2016 to April 2017, the spacecraft executed 20 near-polar orbits that passed just outside the outer edge of the main rings; these "Ring-Grazing Orbits" (RGOs) provided the mission's best viewing of the A and F rings, the Cassini Division, and the outer B ring. From April to September 2017, the spacecraft is executing 22 near-polar orbits that pass between the innermost D ring and the planet's clouds; this "Grand Finale" (GF) provides the mission's best viewing of the C and D rings and the inner B ring.

2. Clumpy Belts

Clumpy structure called "straw" was previously observed in parts of the main rings [1], especially in the troughs of density waves and in other locations where ring material has recently been released from compression. RGO images show this structure with greater clarity, which will enable measurement of the structure and comparison with numerical simulations.

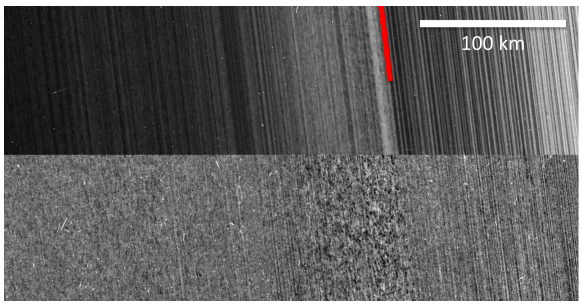

Figure 1: Cassini image of strong radial structure in the inner A ring. The upper panel shows the plain image, while the lower panel shows a contiguous portion of the same image after application of a filter that removes the radial structure so that compact structure is more visible. The red line marks a boundary between two characters of radial structure.

More surprisingly, RGO images reveal similar clumpy belts in regions that (to our knowledge) have *not* recently undergone compression, such as the inner A ring (Fig. 1). This region is thought to be subject to self-excited modes called "viscous overstability" [2], though it is not yet clear whether the clumpy belts are correlated with the occurrence of VO.

3. Flocks of Propellers

A "propeller" is a local disturbance in the ring created by an embedded moon [3, 4, 5]. Cassini has observed two classes of propellers: small propellers that swarm in the "Propeller Belts" of the mid-A ring (discussed in this section), and giant propellers whose individual orbits can be tracked in the outer A ring (discussed in the following section).

The original discovery of propellers in the Propeller Belts [3] used four images taken from unusually close range during Cassini's maneuver to initially put itself into Saturn orbit in 2004. The propellers discovered in those images were smaller than those seen later in the mission in the same location [4, 5], and a clear connection between the different size populations has

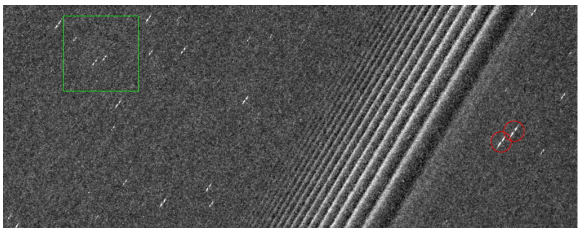

Figure 2: Cassini image of propellers and a density wave in the mid-A ring. The green square indicates the approximate size of the original propeller discovery images [3], and the propellers within the green square are approximately the size of the discovery propellers. The red circles indicate larger propellers nearby.

not previously been established. RGO images (e.g., Fig. 2) show, for the first time, a wide range of sizes in the Propeller Belts, putting the SOI propellers in context.

4. Propeller Close-ups

The orbits of giant propellers have been tracked for the past decade, tracing the effect that the ring has upon them [6]. In the RGOs, close-up views of selected propeller shed light on their effects upon the ring.

We will present maps of of the propeller structures, with enhanced ability to convert brightness to optical depth and surface density due to information from both the lit and unlit sides of the rings (Fig. 3). The images contain more complex structure than is predicted by simple models, which we will describe, and for which we will comment on likely explanations.

5. Impact Ejecta Clouds

Being a large and delicate system, Saturn's rings function as a detector of the planetary environment. The population of decimeter-to-meter-sized meteoroids in Saturn's vicinity was estimated from images of impact ejecta clouds in the rings [7]. RGO images increase the number of detected IECs by a factor of several. Also, spectral information from color filters may constrain the particle-size distribution of the ejecta, thus constraining the fracture properties of ring material.

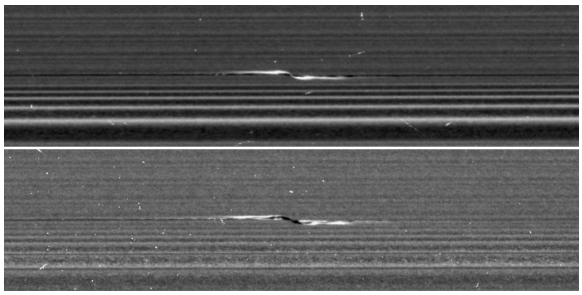

Figure 3: The propeller "Santos-Dumont," viewed on the lit side (top) and unlit side (bottom) of the rings. On the lit side, the rings look darker where there is less material to reflect sunlight. On the unlit side, some regions look darker because there is less material, but other regions look dark because there is so much material that the ring becomes opaque. For example, in the unlit-side view, the broad, dark band through the middle of the propeller seems to be a combination of both empty and opaque regions.

References

[1] Porco, C.C., et al. 2005. Cassini imaging science: Initial results on Saturn's rings and small satellites. Science 307, 1226-1236.

[2] Rein, H., and H.N. Latter 2013. Large-scale N-body simulatiosn of the viscous overstability in Saturn's rings. MNRAS 431, 145-158.

[3] Tiscareno, M.S., et al. 2006. 100-meter-diameter moonlets in Saturn's A Ring from observations of 'propeller' structures. Nature 440, 648-650.

[4] Sremčević, M., et al. 2007. A belt of moonlets in Saturn's A ring. Nature 449, 1019-1021.

[5] Tiscareno, M.S., J.A. Burns, M.M. Hedman, and C.C. Porco 2008. The population of propellers in Saturn's A Ring. Astron. J. 135, 1083-1091 (arXiv:0710.4547).

[6] Tiscareno, M.S., R.P. Perrine, D.C. Richardson, M.M. Hedman, J.W. Weiss, C.C. Porco, and J.A. Burns 2010. An analytic parameterization of self-gravity wakes in Saturn's rings, with application to occultations and propellers. Astron. J. 139, 492-503 (arXiv:0911.3161).

[7] Tiscareno, M.S., et al. 2013. Observations of ejecta clouds produced by impacts onto Saturn's rings. Science 340, 460-464.

EPSC Abstracts
Vol. 11, EPSC2017-1009-1, 2017
European Planetary Science Congress 2017

Compositional 3-D mapping of icy dust grains in the E-ring

L. Nölle (1), F. Postberg (1), N. Khawaja (1), T. Albin (2) and R. Srama (2)
(1) Institute of Earth Sciences, Heidelberg University, Germany, (2) Institute of Space Systems, Stuttgart University, Germany (Lenz.Noelle@geow.uni-heidelberg.de)

Abstract

Compared to the inner rings, which are very narrow and well defined around the equatorial plane of Saturn, the E-ring is very diffuse with no strict boundaries because many dust particles, moving on various inclined orbits around Saturn, are blurring the structural limits of the ring. Cassini's Cosmic Dust Analyser (CDA) provides a large number of time-of-flight mass-spectra of dust impacts recorded during a planar E-ring passage in 2015, which extract the chemical composition of dust grains. During these measurements the boresight of the CDA was periodically changed in vertical direction to allow the examination of not only the radial but also the vertical compositional distribution of the incoming dust grains. Here we present the first radial and vertical, compositional profiles of dust grains within the E-ring and discuss the implications.

EPSC Abstracts
Vol. 11, EPSC2017-1010-1, 2017
European Planetary Science Congress 2017

Reproducing impact ionization mass spectra of E and F ring ice grains at different impact speeds

F. Klenner, R. Reviol and F. Postberg
Institute of Earth Sciences, Heidelberg University, Germany (Fabian.Klenner@geow.uni-heidelberg.de)

Abstract

In situ mass spectrometers analyzing the composition of icy grains in space, like the Cosmic Dust Analyzer (CDA) on Cassini or the Surface Dust Analyser (SUDA) onboard the future Europa Clipper Mission, employ the impact ionization mechanism to ionize substantial parts of impinging ice grains by the kinetic energy of the impact. As the impact speed of the grains can vary greatly, the resulting cationic or anionic mass spectra can have very different appearances, even if similarly composed.

A good analog to the impact ionization of ice grains is a laser based analog experiment where a μm sized liquid water beam is intersected by a pulsed infrared laser at suitable energies and wavelengths. The cationic and anionic products are monitored by a high performance time of flight mass spectrometer. In this way, CDA's cationic mass spectra from ice grains of the E ring as well as the F ring could be accurately reproduced.

In this work, we demonstrate the capability of our improved laser experiment in Heidelberg to quantitatively reproduce CDA spectra recorded at a wide variety of impact speeds. CDA spectra of E and F ring ice grains recorded at different impact speeds varying from 4 – 20 km/s are grouped into different speed regimes. We accurately reproduce the drastically varying spectral appearances by tuning the laser parameters and the delaytime of the gating system in front of the mass spectrometer. We compare CDA spectra of different composition (Type 1, 2, and 3 from Postberg et al., 2008, 2009) recorded at the different speed regimes with our analog spectra and prove the capability of the Heidelberg analog experiment to reproduce them.

References

[1] Postberg, F., Kempf, S., Hillier, J., Srama, R., Green, S., McBride, N and Grün, E.: The E-ring in the vicinity of Enceladus II. Probing the moon's interior-The composition of E-ring particles, Icarus, Vol. 193, pp. 438-454, 2008.

[2] Postberg, F., Kempf, S., Schmidt, J., Brilliantov, N., Beinsen, A., Abel, B. Buck, U. and Srama, R..: Sodium salts in E-ring ice grains from an ocean below the surface of Enceladus, Nature, Vol. 459, pp. 1098-1101, 2009.